ACS APPLIED MATERIALS & INTERFACES

Research Article

www.acsami.org

Strategies for Replicating Anatomical Cartilaginous Tissue Gradient in Engineered Intervertebral Disc

Maumita Bhattacharjee,[†,‡] Shibu Chameettachal,[†] Shikha Pahwa,[†,‡] Alok R. Ray,[‡] and Sourabh Ghosh*[,†]

[†]Department of Textile Technology, Indian Institute of Technology, New Delhi, India

[‡]Centre for Biomedical Engineering, Indian Institute of Technology and All India Institute of Medical Sciences, New Delhi, India

ABSTRACT: A critical challenge in fabricating a load bearing tissue, such as an intervertebral disc, is to simulate cellular and matrix alignment and anisotropy, as well as a specific biochemical gradient. Towards this goal, multilamellar silk fibroin scaffolds having criss-cross fibrous orientation were developed, where silk fibers in inner layers were crosslinked with bioactive molecule chondroitin sulfate. Upon culturing goat articular chondrocytes under static and dynamic conditions, lamellar scaffold architecture guided alignment of cells and the newly synthesized extracellular matrix (ECM) along the silk fibers. The dynamic culture conditions further improved the cellular metabolic rate and ECM production. Further the synergistic effect of chemical composition of scaffold and hydrodynamic environment of bioreactor contributed in developing a tissue gradient within the constructs, with an inner region rich in collagen II, glycosaminoglycan (GAG), and stiffer in compression, whereas an outer region rich in collagen I and stiffer in tension. Therefore, a unique combination of chemical and physical parameters of engineered constructs and dynamic culture conditions provides a promising starting point to further improve the system towards replicating the anatomical structure, composition gradient, and function of intervertebral disc tissue.

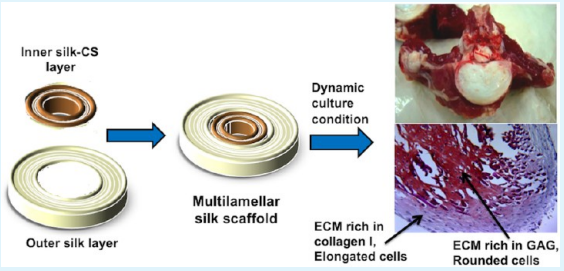

KEYWORDS: *intervertebral disc, cartilaginous tissue gradient, dynamic culture, shear forces, silk fibroin, chondroitin sulfate*

1. INTRODUCTION

Intervertebral disc (IVD) is a complex load bearing tissue having unique structure and composition with characteristic regional variation in multi-lamellar annulus fibrosus (AF), surrounding the nucleus pulposus (NP).[1] Based on differences in matrix composition and cellular phenotypes, the lamellae of AF can be further distinguished into the peripheral fibro-cartilaginous outer AF layers and inner AF layers. Progressing from outer AF towards NP region, expression of collagen type I decreases and collagen type II and proteoglycan increases. The layers in inner AF are thicker than outer AF layers and less hydrated in comparison with NP.[2,3] In outer AF, elongated cells are aligned parallel to collagen I fibers, whereas inner AF consists of spherical cells embedded within the extracellular matrix (ECM).[4]

Such regional distinction in cellular morphology and ECM composition play an important role in managing compressive and tensile loads in spinal joints.[4] Under physiological loading of IVD, the NP applies outward pressure to AF. A study by stress profilometry revealed that the stress on the different anatomic zones of IVD are different.[5] The outer AF zone resists large tensile stresses generated along circumferential and radial direction, but shares smaller compressive stress. In comparison, the inner AF provides resistance against major proportion of compressive loads.[5] Under tensile loading, the elongated outer AF cells exhibit larger strain concentrations and volume increase under both ramp and relaxation. In contrast, the NP cells manifest minimal volumetric changes with large hydrostatic pressures.[6,7] The presence of a dense collagen filamentous network in the outer AF tissue imparts reduced bulging during compression, bending, and torsional loading of the disc. On the other hand, comparatively less dense collagenous matrix and the proteoglycans of inner AF absorb large compressive deformations by generating hydrostatic swelling pressure and dissipate load uniformly.[8] Hence successful engineering of a complex load bearing disc tissue would demand recapitulation of both ECM organization and composition, by simulating the unique orientation of collagen fibers within the outer layers and the proteoglycan enriched matrix within the inner layers. Most of the previous attempts[8−10] to develop tissue engineered IVD failed to accumulate enough ECM proteins leading to inferior mechanical properties, and to recreate anatomical cartilaginous tissue gradient akin to native AF tissue, which would be critically required to govern the differential mechanical behavior of the AF tissue.

In an attempt to regulate ECM production of outer and inner AF cells by mechanical stimulus, the outer and inner AF cells were seeded on fibrous poly(glycolic acid)-poly(L-lactic acid) scaffolds and subjected to hydrostatic pressure of 5 MPa at 0.5 Hz.[11] Under hydrostatic pressure both outer and inner AF cells proliferated, while outer AF cells extensively infiltrated into the interior of the constructs at 5 MPa pressurization. Hydrostatic

Received: September 5, 2013
Accepted: December 16, 2013
Published: December 16, 2013

pressurization showed no effect on collagen I production; however, significant increase in collagen II in both cell types was observed with uniform distribution under dynamic loading. The limitations of the study were the absence of cartilaginous gradient formation and lack of studies on mechanical properties.[11] In another study, a biphasic scaffold was developed using demineralized bone matrix gelatin for outer layers and poly(caprolactone triol malate) which were orientated in concentric sheets for the inner layer. Although the constructs could emulate the biochemical composition to some extent, they failed to replicate the unique structural hierarchy of the native AF tissue and hence demonstrated lower mechanical strength as compared to the native tissue.[12]

To develop a scaffold matching the dimensions of a native disc tissue, we developed silk fiber-based multilamellar scaffolds wherein the silk fibers were arranged parallel to each other at a specified angle in one layer and opposite angles in successive layers,[13] surrounding the inner silk fibroin hydrogel. Such lamellar scaffold allowed abundant amount of glycosaminoglycan (GAG) and collagen deposition by human nasal chondrocytes and also achieved mechanical parity with the goat AF tissue within 4 weeks under uniaxial compression loading.[14] The goal of the present study was to simulate anatomically relevant AF tissue gradient within same construct; thus, the outer layers of the scaffolds simulated the structural organization of outer AF layer while the inner silk layers were crosslinked with chondroitin sulphate. The scaffolds were cultured with articular chondrocytes for 4 weeks under static and dynamic culture which could generate an outer AF layer containing mainly collagen I and an inner layer rich in collagen II and GAG simulating the ECM organization, composition, and mechanical behavior of the AF part of the disc tissue.

2. EXPERIMENTAL SECTION

2.1. Preparation of Lamellar Fibrous Scaffolds: Outer Silk and Inner Silk-CS Scaffolds. The *Antheraea mylitta* silk fibers were procured from the local textile industry and were degummed by boiling in 0.02 M Na_2CO_3 for 30 minutes so as to separate the outer sericin layer of silk. The remaining silk fibroin fibers were thoroughly rinsed in deionized water. The silk fibers were then dried at 40°C in an oven, and scaffolds were fabricated using the custom made winding machine.[13,14] The outer layer was made up of only silk fibers which were aligned parallel to each other at a defined angle of 30° to the vertical axis in one layer and oriented in the opposite direction in successive layers simulating the specialized collagen fiber orientation within the outer AF tissue. The inner layer was made of silk fibers crosslinked with Chondroitin-4-sulphate (CS), as mentioned earlier,[14] to mimic the structure and composition of the inner AF layers. Briefly, 6 % of CS was first oxidized by mixing 6% of sodium periodate to it in dark condition to form aldehyde groups. Silk fibers were then dipped in oxidized CS solution in the ratio of 1:1. Silk fibroin contains about of 5% of Arginine residues whose amine groups interacts with aldehyde groups of oxidized CS to form Schiff's base.[14] The inner silk-CS ring was then inserted onto the outer silk ring, and the scaffolds were 0.3 cm thick and 1 cm wide.

2.2. Cell Culture. Chondrocytes were isolated from goat articular cartilage, as previously described.[15] Briefly, remnants of articular cartilage were incubated for 16 h at 37 °C in 0.1% type II collagenase (Gibco) followed by filtration of cell suspension through a 70 μm sterile mesh, and then resuspended at a density of 6000 cells/cm^2 in Dulbecco's modified Eagle's medium (Cellclone) containing 10% fetal bovine serum (Biological industries), 100 U/ml penicillin-streptomycin, 2.5 μg/mL Gentamycin, and 5 μg/mL amphotericin, 5 ng/mL FGF-2 (Millipore), and 1 ng/mL TGF β1 (Millipore). Prior to cell culture, scaffolds were sterilized by overnight incubation at 70% ethanol and pre-wet in complete medium. Chondrocytes (P1) were manually seeded by pipetting 2×10^5 cells on the outer silk ring and 2×10^5 cells on the inner silk-CS ring separately and cultured statically for one day. The inner silk-CS ring was then inserted onto the outer silk ring and then some of the scaffolds were transferred to a flat bottomed spinner flask (Bellco, U.S.A.) containing 100 mL of media for dynamic culture. The scaffolds were fixed to stainless steel wires attached to the top of the flask. The bioreactor was placed within an incubator with 5% CO_2 and stirring speed was set to 90 rpm using a 4 cm long magnetic bar. Constructs were cultured under static and dynamic conditions in complete medium (Dulbecco's Modified Eagle's medium supplemented with 10% fetal bovine serum, 100 U/ml penicillin-streptomycin, 2.5 μg/mL Gentamycin and 5 μg/mL amphotericin, 1 ng/mL TGF β1). The medium was changed twice a week. Constructs were harvested after 1 day, 2 weeks, and 4 weeks for analysis.

2.3. Metabolic Activity. Metabolic activity was determined using the MTT assay. Constructs harvested after 1 day, 2 weeks, and 4 weeks were rinsed in PBS and stained with tetrazolium salt MTT for up to 4 h at 37°C. The constructs were then dipped in equal volume of dimethylsulfoxide (DMSO) to dissolve the crystals. Reading was taken at 570 nm (n = 4, each experiment was repeated twice) using iMark microplate Absorbance reader (Biorad).

2.4. Biochemical Analysis. Constructs (n = 4, each experiment was repeated twice) were digested with proteinase K solution. GAG content was measured spectrophotometrically after reaction with dimethylmethylene blue, with chondroitin sulfate (from bovine trachea, MW 10^5 Da., Sigma) as a standard.

Total collagen was measured by hydroxyproline assay. Constructs were digested with 500 μL of 1 mg/mL proteinase K (including proteinase inhibitor) and incubated overnight at 56°C. The temperature was increased to 100°C and allowed to boil for 10−15 min. Samples were then hydrolyzed by adding 1.5:1 volume ratio of 6 N HCl and incubated over night at 110 °C. The samples were dried and analyzed using hydroxyproline assay with hydroxyproline as a standard (n = 3, each experiment was repeated twice).[16]

2.5. Histological and Immunohistochemical Analysis. Human AF tissue was obtained after dissection from a 56 year-old female patient with informed consent at University Hospital, Basel, Switzerland.[14] Constructs were rinsed with PBS, fixed in 4% formalin, embedded in paraffin, cross-sectioned (7 μm) and stained with H&E and Safranin-O.

Constructs were processed for immuno-histochemistry by first rinsing in PBS thrice. Constructs were then fixed in 4% formalin for 4 h and washed in PBS thrice. Constructs were permeabilized with triton X (0.1%), followed by PBS washing for three times. Constructs were then blocked with BSA (1%)/PBS followed by PBS washing for three times. Constructs were then incubated with primary antibodies: Anti-elastin (4 μg/mL, 1:200, Millipore), Anti-collagen I (4 μg/mL, 0.2:100, Millipore) and Anti-collagen II (200 μg/mL, 1:100, Millipore), Goat anti-mouse IgG Antibody-FITC conjugate (1:200, Millipore), Alexa Fluor 546 Goat Anti-Mouse IgG (1:200, Invitrogen) by incubating for 1 h at room temperature. Nuclei were stained using DAPI (300 nM, 2:100, Invitrogen) for 5 minutes at room temperature. Images were captured using a confocal microscope (Leica TCS SP5) by scanning the constructs upto 40 μm from periphery. The images of each layer were then stacked together to get a composite image.

The collagen fiber alignment was quantitatively measured using ImageJ plug-in "OrientationJ",[17] to measure the directional coherency coefficient of the collagen fibers at various regions (9 regions randomly selected per sample) of human AF tissue and tissue engineered construct. A coherency coefficient close to 1, represents strong coherent orientation of the native fibers along the ellipse long axis. A coherency coefficient close to zero, indicates random orientation of the fibers.

2.6. Gene Expression Studies. Total RNA was isolated from engineered constructs using Rneasy mini kit (Qiagen) according to supplier's instruction. RNA concentrations and the purity were determined using a Nanodrop 2000C (Thermo Scientific, Wilmington, DE, U.S.A.). Extracted RNA was reverse-transcribed into cDNA using first strand cDNA Synthesis Kit (Fermentas). Quantitative real-time

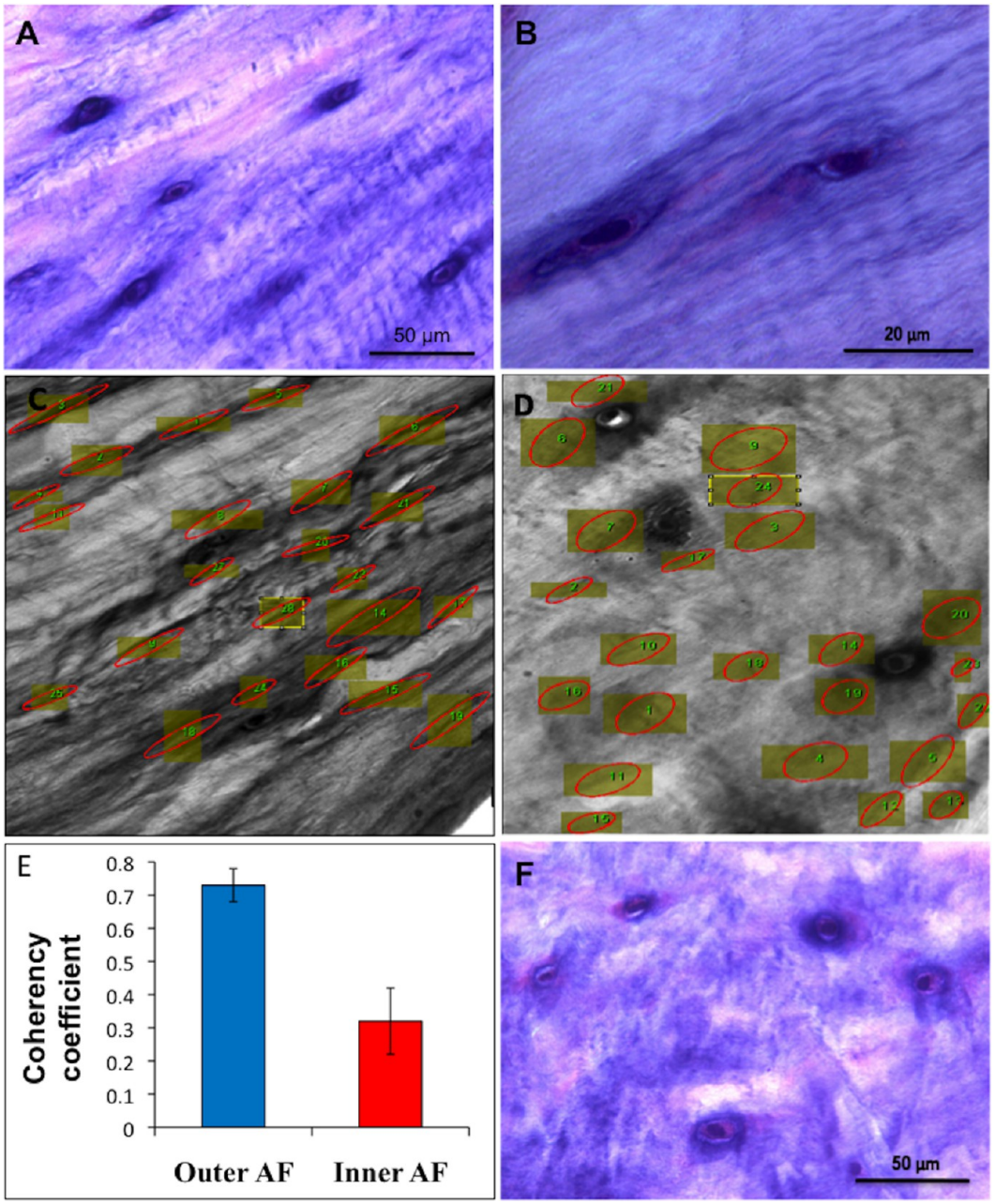

Figure 1. (A) H&E staining showing elongated cells on the outer AF layer. (B) Magnified view of outer AF region showing highly organized alignment of fibrous ECM. (C,D) Coherency coefficients calculation from the outer and inner AF regions (red ellipses inside the yellow region of interest). (E) Comparative coherency coefficients values of outer and inner AF region. (F) H&E staining showing spherical cells on the inner AF layers.

RT-PCR was conducted using SYBR Green Master Mix and Rotor gene Q thermocycler (Qiagen). The reactions were carried out in triplicate in 25 μL total volume containing 1 μL cDNA and 2.5 μL primers. The Assay-on-demand (Qiagen) primers used were GAPDH (Cat no. QT00079247), Aggrecan (Cat No. QT00001365), Collagen I (Cat no. QT00037793), Collagen II (Cat no. QT00049518), Sox-9 (Cat no. QT00001498), Biglycan (Cat no. QT01870029), Elastin (Cat no. QT00034594). The analysis was carried out with the Rotor gene Q software and the relative expression levels were calculated using the $2^{-(\Delta\Delta c(t))}$ method with GAPDH as a control. Three samples from each condition were evaluated, and each experiment was repeated twice.

2.7. Mechanical Characterization. After 4 weeks of culture in static and dynamic condition, the outer and inner layers were separated from each other and assessed for uniaxial tensile and unconfined compressional properties. Compression modulus of 4 weeks cultured constructs were carried on a computer-controlled Universal Testing Machine (UTM) model H5KS (Tinius Olsen, single stand machine, England) with QMAT 5.37 professional software. The samples (n = 3, each experiment was repeated twice) were clamped on to the jaws of the UTM and compressive load of up to 900 N was applied with a test speed of 1 mm/min and compressed to 20% strain with a preload of 0 N. The tensile strength of the engineered constructs (n = 3, each experiment repeated twice) were tested using the same machine as described above. The instrument was equipped with 900 N load cell with a gauze length of 15 mm. Strain rate of 1 mm/min was applied and tested for tension to failure. Statistical significance was calculated with $p < 0.05$ as the significant criteria.

2.8. Statistical Analysis. Statistical significance was calculated by independent t tests where two independent variables or data groups were used and ANOVA where differences between multiple variables

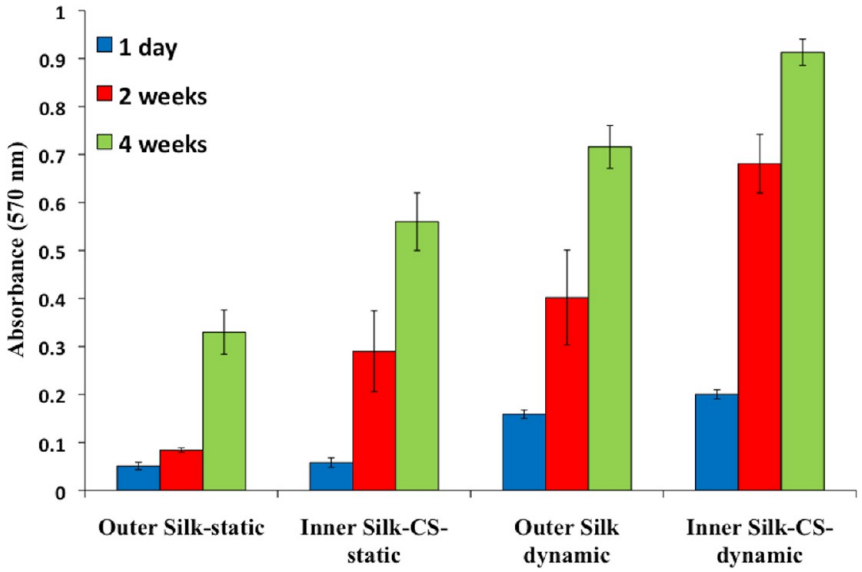

Figure 2. MTT assays of the constructs including outer silk ring and inner silk-CS ring cultured under static and dynamic conditions after 1 day, 2 weeks, and 4 weeks. The cell metabolic activity was found to be significantly higher ($p < 0.05$) in constructs under dynamic conditions as compared to static environment after 4 weeks.

were compared using SPSS 17 software (SPSS Inc., an IBM Company, Chicago, U.S.A.) and was considered significant at $p < 0.05$.

3. RESULTS AND DISCUSSIONS

3.1. Anatomical Organization of AF Tissue. The mechanical function of the AF tissue is governed by the regional variation within the AF layer. Hence anatomical features should be studied to elucidate the role of regional difference in structure-property relationship in the AF layer. The H&E stained sections of outer and inner AF layers showed distinct regional variation between these two layers of AF in terms of cell morphology; the cells in the outer AF layer were elongated and were aligned parallel to the collagen fibers (Figure 1A, B) whereas the inner AF layer was dominated by spherical cells as shown in Figure 1F.

The alignment of collagen fibers were measured using orientationJ.[17] Figure 1C and D showed the coherence in the collagen fiber orientation, as indicated by red ellipses within the yellow region of interest. The coherency coefficient for the inner AF region was found to be 0.32 ± 0.1 showing heterogenous/disperse collagen fiber orientation, whereas the outer AF region showed coherency coefficient 0.73 ± 0.05 (Figure 1E), indicating a dominant orientation/strong structural organization of the collagen fibers.[17]

To replicate such regional distinction of outer and inner AF layer, we developed multi-lamellar silk scaffolds with an outer silk layer (containing 25 layers) and inner silk layer (containing 25 layers), but inner layers were conjugated with CS. Silk was chosen because of its extraordinary mechanical properties. In native disc, GAG content increases while moving from outer AF towards inner AF.[18,19] Chondroitin sulfate was reported to enhance chondrogenic gene expression and matrix production. In our previous study[14] a culture of human nasal chondrocyte over silk fibrous scaffold, crosslinked with Chondroitin-4-sulfate (C-4-S), resulted in the synthesis and accumulation of abundant amount of GAG within the construct. Moreover, C-4-S was chosen as it is the predominant CS isomer in embryonic or neonatal discs, whereas C-6-S is predominating in the adult discs. Earlier reports have shown that the ratio of 6- to 4-sulphated N-acetylgalactosamine residues increases with age[20] and thus we anticipate that engineered AF construct having C-4-S may prevent degeneration to some extent because of its reported therapeutic effects.

3.2. Effect of Flow Conditions in Modulating Cellular Behavior to Form AF Tissue Gradient. The scaffolds were cultured with goat articular chondrocytes up to 4 weeks and cultured under static conditions, as well as dynamic condition using a spinner flask bioreactor. The rotational speed of the magnetic stirrer bar was set to 90 rpm, because an earlier study[21] reported enhanced collagen production at 90 rpm compared to other rotational speeds (60 and 120 rpm). Less amount of collagen was deposited at the 60 rpm, whereas 90 and 120 rpm resulted in similar collagen content.[21]

To estimate the metabolic activity of cells under static and dynamic conditions the two layers (outer unconjugated silk and inner silk-CS regions) were separated from each other and analyzed by MTT assay. As expected, after 1 day culture, the chondrocytes exhibited similar level of metabolism (statistically no significant difference) in both outer silk and inner silk-CS constructs under static conditions. But under dynamic culture condition, the cellular metabolic rate increased 1.2 times in inner silk-CS as compared to outer silk ring, which in turn were higher than the metabolic activity in constructs cultured under static conditions. After 4 weeks under static conditions, 1.6 fold higher cellular metabolism was observed in inner silk-CS ring as compared to outer silk layers, whereas under dynamic condition the cellular metabolism increased 1.3 times in inner silk-CS ring (significant at $p < 0.05$) as compared to outer silk ring. After 4 weeks two fold (significant at $p < 0.05$) increase was observed in constructs (outer silk and inner silk-CS ring) under dynamic conditions as compared to the static culture (Figure 2). Taken together, under dynamic culture cells showed higher metabolic activity as compared to under static culture at every time point (day 1, week 2, and week 4), probably because of the enhanced mass transport of nutrients and gases in the dynamic culture condition.[22] In the static culture, limited diffusion of nutrients and gases resulted in a lower metabolic rate. But the synergistic activity of the dynamic culture

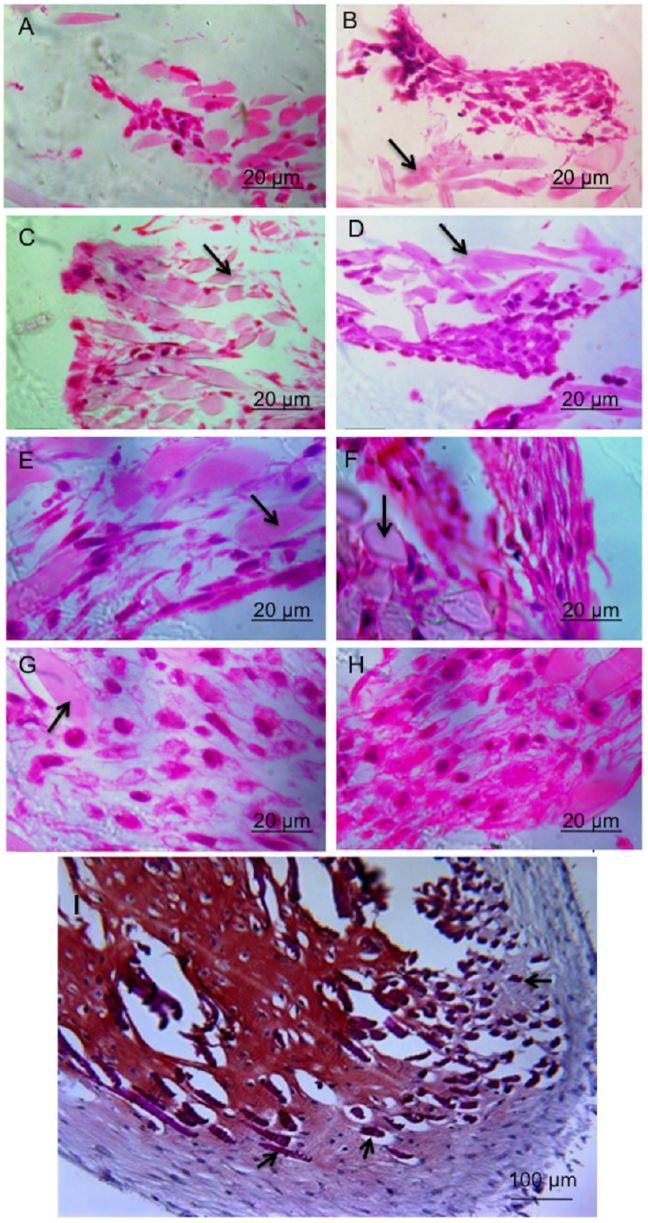

Figure 3. H&E staining (A–H): (A) Outer silk showing some elongated and some round cells after 2 weeks under static conditions. (B) Outer silk showing mostly rounded cells after 4 weeks under static conditions. (C) Inner silk-CS showing some round cells after 2 weeks under static conditions. (D) Inner silk-CS showing increased number of rounded cells after 4 weeks under static conditions. (E) Outer silk showing elongated cells after 2 weeks under dynamic conditions. (F) Outer silk showing elongated cells after 4 weeks under dynamic conditions. (G) Inner silk-CS showing some round cells after 2 weeks under dynamic conditions. (H) Inner silk-CS showing increased number of rounded cells after 4 weeks under dynamic conditions. (I) Safranin-O staining demonstrated tissue gradient formation; uniform and intense GAG staining in the inner silk-CS region with no GAG staining in the outer silk region under dynamic conditions after 4 weeks. (Arrows indicate silk fibers).

condition and chemical conjugation with CS appeared to be the best metabolic regulator for cellular growth.

To investigate whether dynamic culture can improve cellular distribution and modulate cellular morphology, the constructs were examined histologically. By 4 weeks of culture, greater number of cells were uniformly distributed in scaffolds when

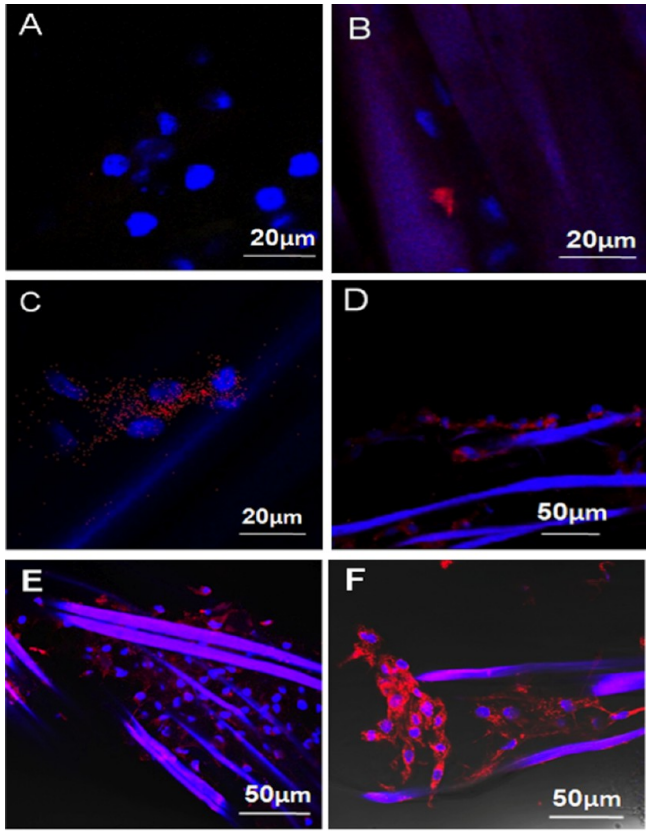

Figure 4. (A) No positive staining for collagen II was visible in the outer silk layer under static conditions after 2 weeks. (B) No staining for collagen II in the outer silk layer under dynamic conditions after 2 weeks. (C) Positive collagen II staining in the inner silk-CS layer under static conditions after 2 weeks. (D) Distinct collagen II fibrous assembly noticed in the inner silk-CS layer under dynamic conditions after 2 weeks. (E,F) Collagen II staining in the inner silk-CS constructs under dynamic conditions after 4 weeks.

cultured in spinner flasks compared to the constructs cultured under static conditions. A regional variation within the cellular morphology was observed within the constructs. The cells in outer silk layers appeared more elongated, as seen in outer AF tissue in vivo,[4] whereas cells in the inner silk-CS layers cultured in the spinner flask appeared rounded akin to the inner AF tissue.[4] Under static condition the cells appeared spherical in both outer and inner layers (Figure 3). After 4 weeks of culture under dynamic condition the engineered constructs showed a clear demarcation in terms of cell morphology, as well as the ECM content, with an inner region uniformly and deeply stained for GAG and an outer region negatively stained for GAG (Figure 3I).

Since safranin-O stained sections demonstrated clear ECM gradient formation, we further investigated how dynamic culture condition might impose localized expression of other ECM proteins, such as collagen I and collagen II. After 2 weeks, nominal to insignificant collagen II staining was observed in the outer silk layer under static and dynamic conditions (Figure 4 A,B). But the silk-CS layer showed positive staining for collagen II under both static (Figure 4C) and dynamic conditions (Figure 4D) with the comparatively higher staining intensity and indication of collagen fibrillar assembly in the silk-CS layer under dynamic conditions. After 4 weeks the intensity of collagen II staining was highest in the inner silk-CS layer

dx.doi.org/10.1021/am403835t | ACS Appl. Mater. Interfaces 2014, 6, 183–193

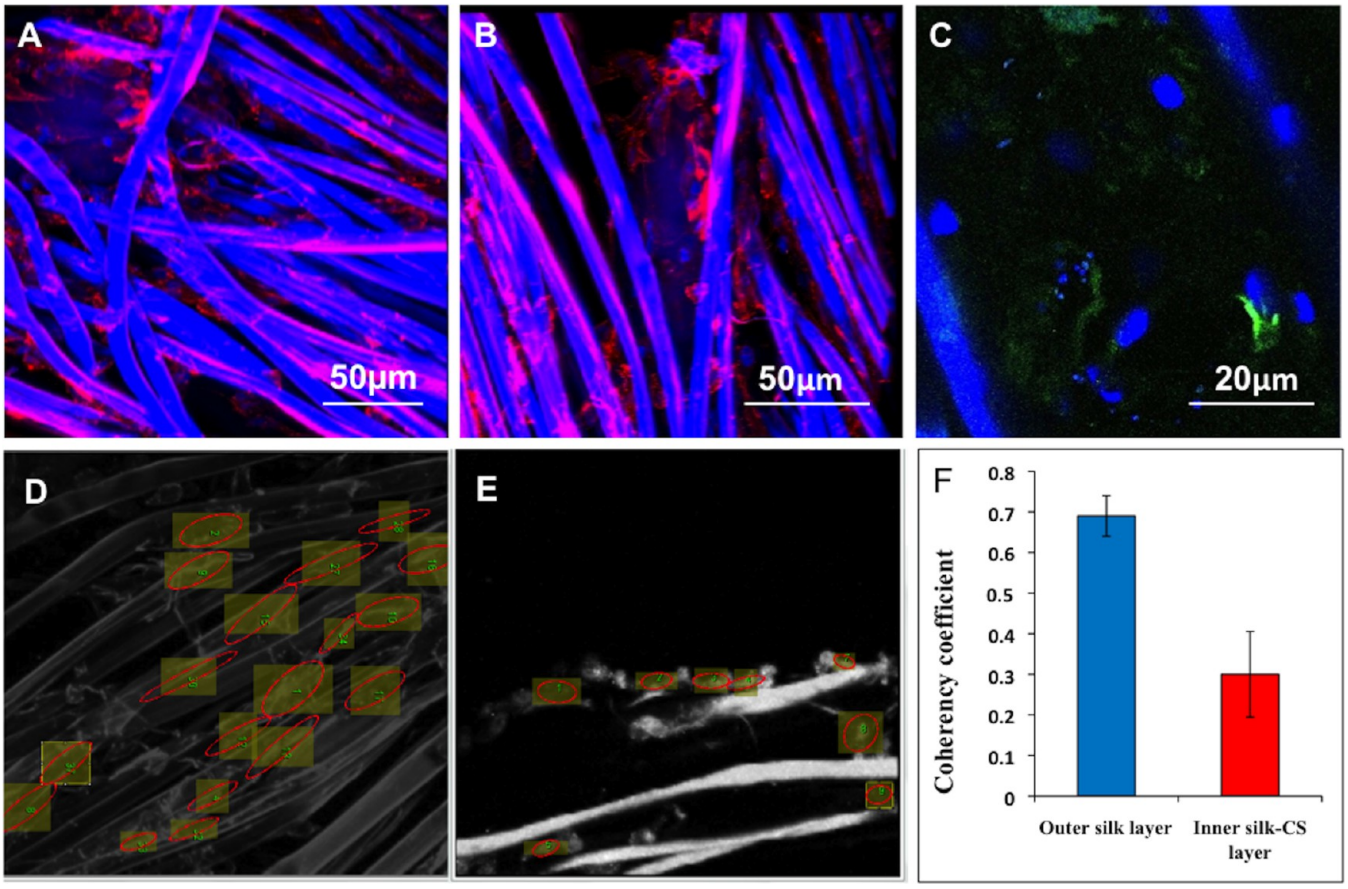

Figure 5. (A, B) Collagen I staining in the outer silk constructs cultured under dynamic condition. (C) Elastin staining in the outer silk layer under dynamic conditions after 4 weeks. (D,E) Coherency coefficient calculations from the outer and inner engineered construct (red ellipses inside the yellow region of interest). (F) Coherency coefficient values of outer and inner engineered construct.

cultured in spinner flasks (Figure 4E,F) as compared to other constructs cultured under static conditions. Collagen I staining was predominant in the outer silk layer (Figure 5A,B) cultured under dynamic condition and was not visible in any other constructs even after 4 weeks.

In vivo, elastin is specifically present parallel to collagen fibers in each lamella in the outer and posterolateral AF tissue, as well as in translamellar crossbridges, running perpendicular to the lamellar plane.[23,24] Elastin helps in recovery of disc after deformation because of large tensile deformations and loading of collagen enriched fibrous ECM.[25] The elastin in the outer AF also helps in attaching the collagenous lamellar layers to the adjacent cartilaginous vertebra body rudiments.[26] After 4 weeks, tropoelastins were found to be assembling or coacervating into microfibrillar elastic fibers, albeit only on cellular surfaces (Figure 5C), only in outer silk layer cultured under dynamic conditions, but not in other conditions. The tropoelastin coacervates while remaining attached to the cell surface integrins and GAG before deposition on microfibrillar bundles.[26,27] Hayes et al.[28] reported punctate amorphous deposition of elastin around a pericellular matrix of annular fibrochondrocytes in the developing outer AF in the bovine model, akin to our findings. However, increasing the culture duration may further enhance the levels of elastin production and self-assembly under dynamic conditions.

The alignment of collagen fibers deposited by the cells in engineered constructs was measured using orientationJ.[17] Figure 5D and E showed the coherence in the collagen fiber orientation, as indicated by red ellipses within the yellow region of interest. The coherency coefficients for the inner silk-CS ring (Figure 5D) was found to be 0.3 ± 0.13 indicating heterogenous/disperse collagen fiber orientation, similar to the inner AF region, whereas the outer silk layer (Figure 5E) showed coherency coefficient of 0.69 ± 0.05, indicating a dominant orientation/strong structural organization of the collagen fibers similar to that of the alignment and anisotropy of ECM in outer AF layers.

In the spinner flask bioreactor, the flow-induced shear force resulted in the formation of elongated cells with higher fractions of collagen I on the outer silk layer. This observation was found to be consistent with earlier reports where bi-zonal constructs were developed simulating the complex structure and function of a meniscus tissue.[29,30] Constructs cultured within a rotary cell culture system facilitated development of bi-zonal tissues with an outer capsule rich in elongated cells and collagen, but lacked GAG. On the other hand, the central region contained a higher fraction of GAG,[29,30] similar to our findings (Figure 3I) where both morphological and biochemical gradient is observed. Another study by Bueno et al. also reported the formation of an outer capsule which showed a strong positive stain for collagen I and negative staining for collagen II under hydrodynamic environment.[31] Further, the hydrodynamic environment and chemical composition of the scaffolds could successfully induce formation of bi-zonal tissues, with an inner region with higher compressive strength and an outer region with higher tensile strength.[22,32] Taken together,

dx.doi.org/10.1021/am403835t | ACS Appl. Mater. Interfaces 2014, 6, 183−193

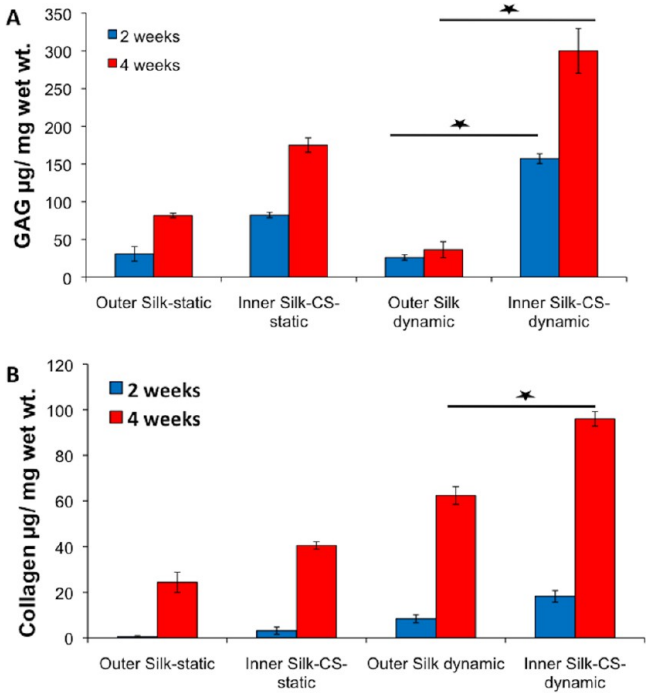

Figure 6. (A) GAG estimation in outer silk and inner silk-CS constructs under static and dynamic conditions. GAG content was found to be significantly higher ($p < 0.05$) in inner silk-CS under dynamic conditions as compared to outer silk layer. (B) Total collagen estimation in outer silk and inner silk-CS constructs under static and dynamic conditions. Collagen content was found to be significantly higher ($p < 0.05$) in outer silk layer under dynamic condition compared to inner silk-CS layer.

the combined effect of hydrodynamic flow, and surface chemistry of the inner silk-CS layer supported rounded cellular phenotype along with the deposition of collagen II and proteoglycans due to the presence of CS, strongly indicating role of scaffold conjugated CS moieties to produce cartilaginous tissue with characteristic morphology, upregulate expression of genes such as sox-9, collagen II, aggrecan, and related ECM production.[33]

Shear forces generated by the spinner flasks have been reported to enhance matrix production in different cell types including epithelial cells,[34] chondrocytes,[35] and AF cells.[36] Earlier studies demonstrated that fluid induced shear stress could increase the secretion of TGFβ1 by the chondrocytes which in turn enhanced cellular proliferation.[37] Further the spinner flask-based culture condition was reported to better control the CO_2, O_2 concentrations and pH of the culture media in comparison to the static environment thereby enhancing the exchange of nutrients, metabolic waste, and dissolved gases.[38] Our observations largely correlate with these studies, that the controlled physicochemical culture parameters offered by spinner flask bioreactor, in combination with strategic chemical functionalization of a scaffold by the bioactive CS molecules, has the potential to modulate cellular morphology, metabolism, and biosynthetic characteristics.

3.3. Biochemical Evaluation of the Gradient Construct. Further the amount of important ECM proteins, like total collagen and GAG, were estimated biochemically at regular time intervals. Production of collagen and GAG was not detectable after 1 week culture. After 2 weeks and 4 weeks, GAG production was found to increase with culture time period in all the conditions. Under static conditions the amount of GAG production was almost double in the inner silk-CS ring as compared to in the outer silk ring. In the spinner flasks GAG production was 7 times higher (significant at $p < 0.05$) in the inner silk-CS layer after 4th week as compared to in the outer silk layer where GAG accumulation was minimal (Figure 6A). There was a nominal amount of collagen produced after 2 weeks by the outer and inner rings under static conditions, whereas almost 6 times higher collagen production was observed (18.28 ± 2.53 μg) in the inner silk-CS ring under dynamic condition as compared to static conditions after 2 weeks. After 4 weeks collagen production was 3 times higher (62.39 ± 3.89 μg) in outer silk rings under dynamic conditions and 2.5 times higher (96 ± 3.16 μg) collagen production was observed in inner silk-CS layer in comparison to constructs under static conditions (Figure 6B). The collagen production was significantly higher in inner silk-CS ($p < 0.05$) as compared to in outer silk layer under dynamic conditions.

Tangential bulk flow[39] in spinner flask bioreactor found to be responsible for the formation of outer collagen rich capsule layer as observed through histology and biochemical evaluation.[31] Interestingly, at higher shear rate (90 rpm) less amount of soluble GAG gets released under culture media. In addition, it has been earlier reported that because of the decreased permeability of the outer capsule in comparison to the top and bottom surface the passage of soluble GAG is blocked and hence their release occurs axially (from top and bottom) and not radially (through the outer layer).[31] Further studies will be conducted if such fibrocartilaginous capsule formation and specific ECM composition may simulate hydraulic permeability of the in vivo AF tissue lamella.

3.4. Effect of Flow Condition on Formation of AF Tissue Gradient Assessed by Gene Expression. Gene expression was studied to assess the localized expression of cartilage specific genes within the constructs. After 2 weeks, sox-9 expressions were found to be similar in outer silk static and dynamic conditions, whereas the inner silk-CS shows 2.3 fold and 2.4 fold higher expression under static and dynamic conditions, respectively. Highest expression of collagen I was observed in outer silk ring under dynamic condition as compared to other condition. Elastin, aggrecan, and biglycan were found to be downregulated in all conditions after 2 weeks. Collagen II expression was found to be highest in inner silk-CS constructs under dynamic culture conditions (Figure 7).

After 4 weeks, sox-9 (22.7 ± 0.99 fold change), collagen II (24.07 ± 0.78 fold change), aggrecan (25.3 ± 3.28 fold change), and biglycan (19.3 ± 1.8 fold change) transcript levels were found to be significantly higher ($p < 0.05$) in the inner silk-CS rings under dynamic conditions as compared to outer silk rings under dynamic conditions. Collagen I and elastin expression increased significantly ($p < 0.05$) in outer silk rings under dynamic conditions as compared to the inner silk-CS rings (Figure 7A–E). Increased collagen I expression is mediated by a potent activator, TGFβ which has been earlier reported to be activated in different cell types (mesangial cells and cardiac fibroblasts) under mechanical forces.[40] The TGFβ signalling required for collagen I expression is mediated by mechanosensitive elements present within the promoter region of collagen I gene, which bind to the major effector molecules Sp1, NF-I, and AP1,[41] and Smad proteins.[42] The molecular mechanism for collagen II expression under mechanical forces was reported by Xie et al.,[43] according to which the proximal region of COL2AI gene promoter contains the binding site for

dx.doi.org/10.1021/am403835t | ACS Appl. Mater. Interfaces 2014, 6, 183–193

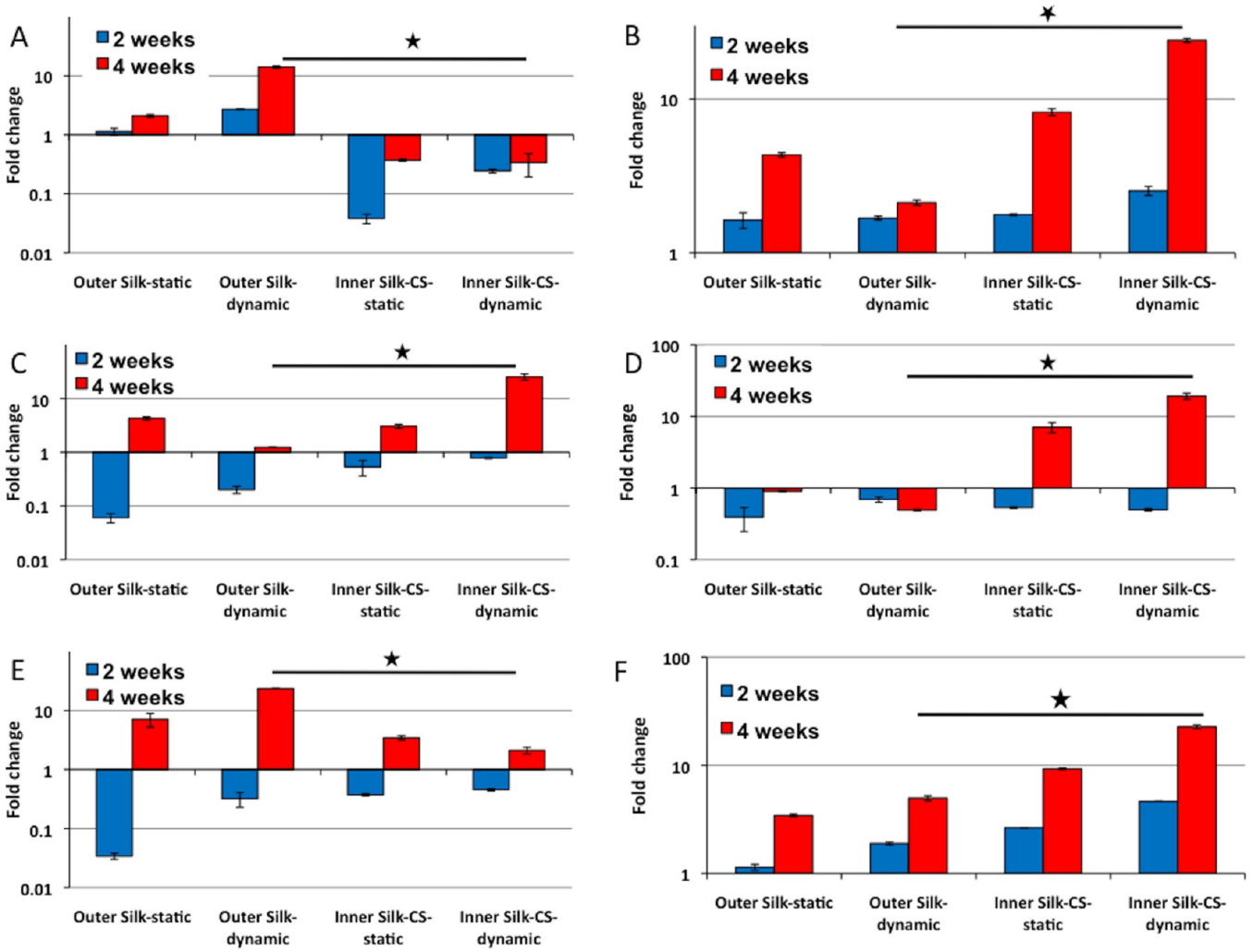

Figure 7. Gene expression studies after the 2nd week and 4th week. (A) Collagen I, (B) Collagen II, (C) Aggrecan, (D) Biglycan, (E) Elastin, (F) Sox-9. Transcript levels of sox-9, collagen, aggrecan were found to be significantly higher ($p < 0.05$) in the inner silk-CS rings under dynamic conditions as compared to all other constructs. Transcript levels of Collagen I and elastin was significantly ($p < 0.05$) higher in outer silk rings under dynamic conditions as compared to the inner silk-CS rings.

transcription factor Sp1 (a zinc finger protein). Sp1 regulates the mechanical forces induced transcriptional activation of collagen II in chondrocytes.[43]

The inner layer showed higher sox-9, collagen II, aggrecan, and biglycan expression both under static and dynamic conditions due to the presence of CS which is known to upregulate chondrogenic transcription factors.[33] Sox-9 is known to be an early chondrogenic marker involved in chondrogenesis. The expression of collagen II represented the formation of inner AF like phenotype within the inner silk-CS layers. Biglycan is a type of small leucine repeat proteoglycans[44] which has been found to be equally present in all zones of the fetal IVD[45] and is known to play an important role in collagen fibrillogenesis.[46] It enhances matrix synthesis by proliferating cells, and its level increases in proliferating cartilage.[45] Reduction in biglycan content leads to increased mechanical stress on IVD, leading to early degeneration.[47] Aggrecan is a member of the proteoglycan family known to bind hyaluronan and imparts the most important hydrodynamic weight bearing properties of the disc tissue.[45] Taken together, the higher transcript levels of collagen II and aggrecan in inner silk-CS region under dynamic conditions indicated the formation of hyaline cartilage-like matrix in the inner side of the construct, whereas higher expression levels of collagen I represented the formation of outer fibrocartilaginous tissue, corroborating findings of histological study and anatomical architecture of AF tissue in vivo.

The outer fibrocartilaginous layer was formed due to the hydrodynamic forces generated within spinner flasks and not because of the non-conjugation of silk fibers with bioactive molecule CS, as the outer silk layer under static conditions was unable to generate elongated cells and collagen I after 4 weeks. Thus the dynamic environment facilitated formation of regional variation similar to the outer AF layer and an inner AF layer of human IVD.

3.5. Regional Variation in the Mechanical Property of the Engineered Constructs. To assess how the regional variation of cellular morphology and ECM content within the constructs could affect their mechanical behavior, the constructs were subjected to uniaxial tensile and unconfined compression loading. It was found that the tensile strength of the outer silk-construct layers was 1.28 fold lower in comparison to inner silk-CS layers under static conditions.

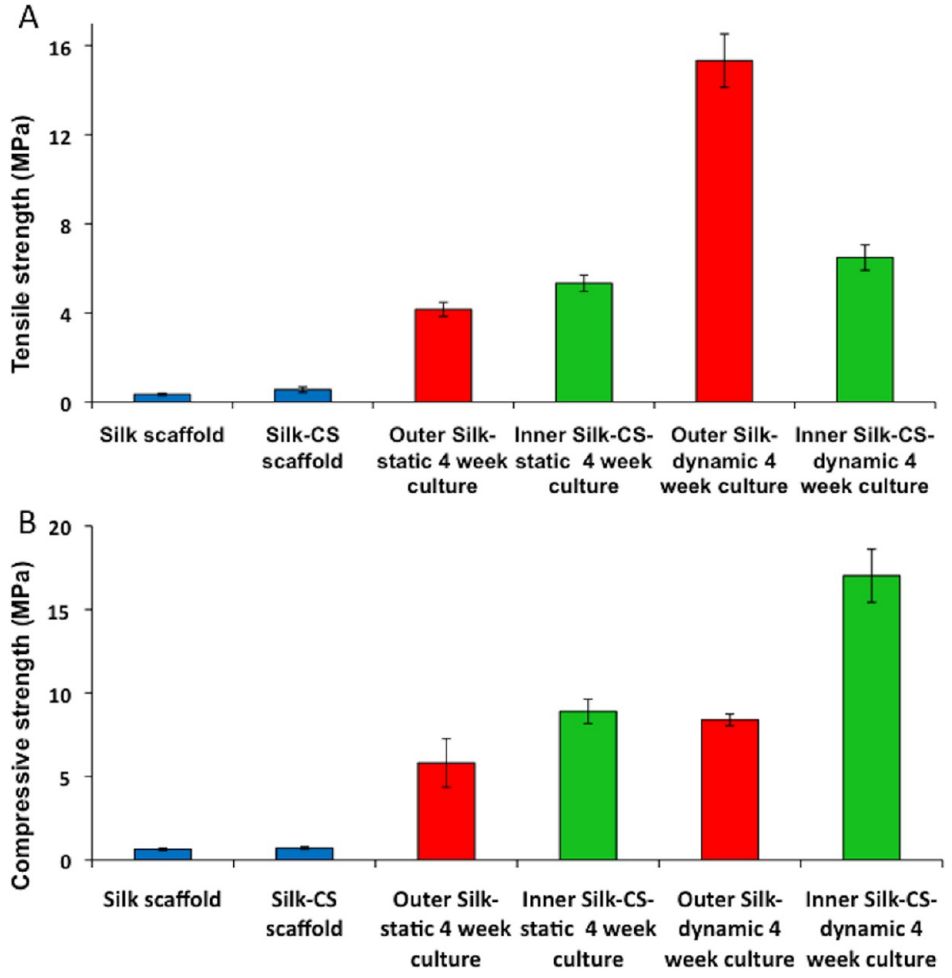

Figure 8. (A) Tensile strength of constructs after 4 weeks. Significantly higher ($p < 0.05$) tensile strength was observed in the outer silk layer as compared to the inner silk-CS layer under dynamic conditions. (B) Compressive strength of constructs after 4 weeks. Significantly higher ($p < 0.05$) compressive strength was observed in the inner-silk layer as compared to the outer silk layer under dynamic conditions.

But the tensile strength of outer silk layer was significantly (2.36 times higher, $p < 0.05$) higher than that of the inner silk-CS layer under dynamic conditions (Figure 8A). The compressive strength of the inner silk-CS was 1.5 fold higher than that of the outer silk ring under static conditions. On the other hand under dynamic conditions the inner silk-CS ring had significantly (1.45 times higher, $p < 0.05$) higher compressive strength than the outer silk ring (Figure 8B).

The inferior mechanical property of the constructs under static conditions is probably due to the lower ECM content. Interestingly, higher tensile strength on the outer ring and higher compressive strength on the inner ring under dynamic conditions represent their potential to resist the complex mechanical loading under in vivo conditions. The higher compressive strength of inner silk-CS ring is due to the accumulation of higher GAG content, and the higher tensile property of the outer layer was due to the collagen accumulation in an organized manner guided by the structural organization of silk fibers.

The higher tensile strength in the outer silk ring under dynamic conditions is consistent with earlier reports where the tensile moduli of the outer AF region were found to be higher as compared to that of the inner AF regions in the human disc.[48] The difference was due to the variation in the biochemical composition showing a decrease in the ratio of types I/II collagen, and an increase in water and proteoglycan content, from outer to inner annulus[48] similar to our findings. The higher tensile properties within the outer layer play an important role in resisting tensile stresses developed as a result of applied compression, bending, or torsional loading and internal swelling pressures[48−50] and also serve to limit the tissue deformation. On the other hand, lower tensile properties of the inner layer make it more deformable during loading therefore facilitating uniform distribution of loads across the inner layers.[48]

In contradiction to our findings, it was reported that the hydrodynamic environment enhanced the production of collagen II and proteoglycans on the superficial layers of tissue engineered cartilage constructs.[51,52] However, the constructs were devoid of collagen I and also lacked deposition of collagen II in the deeper layers. Moreover the production of these important ECM proteins failed to achieve functional equivalence to the native tissue.[50,51] On the other hand, our study demonstrated that the constructs cultured under dynamic conditions displayed anatomically relevant bizonal cartilaginous structure. Dynamic environment generated shear forces resulting in an outer layer having elongated cells which expressed collagen I leading to enhanced tensile strength and the inner silk-CS layers (due to the CS-conjugation to silk fibrous matrix) containing rounded chondrocytes with

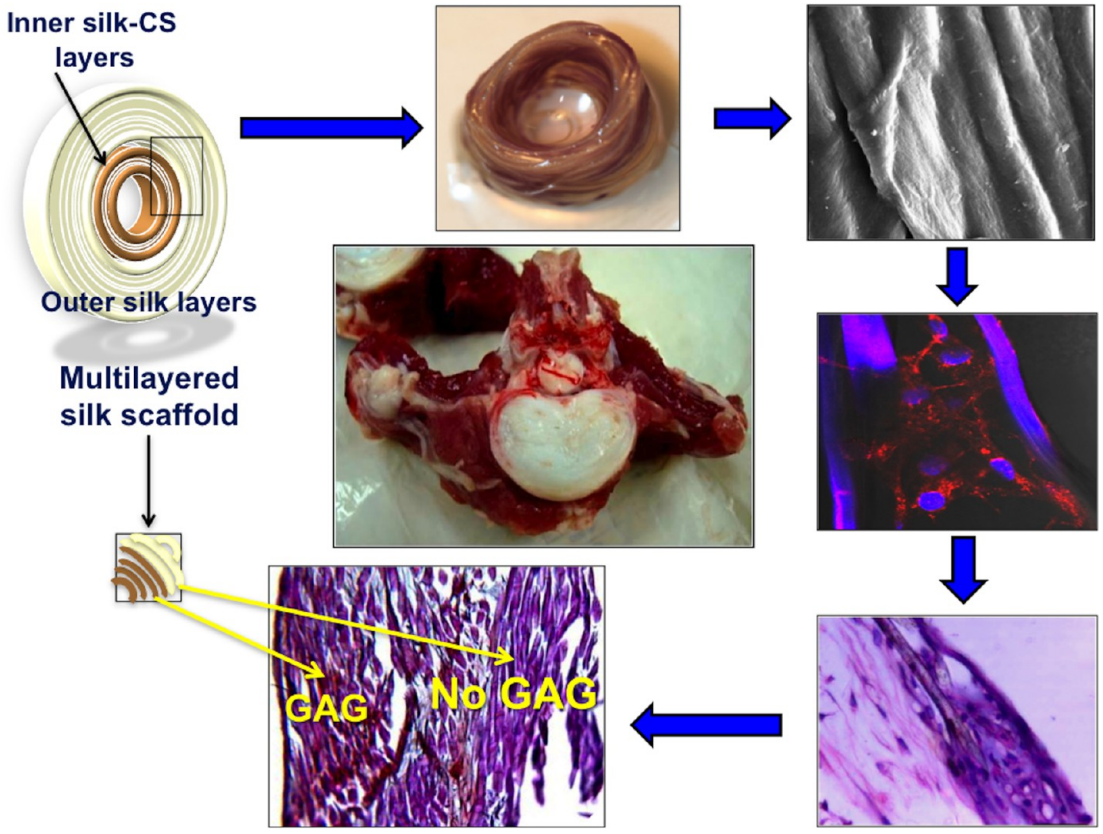

Figure 9. Schematic diagram highlighting differences in outer and inner layers of the multi-lamellar constructs: Dynamic culture condition generated shear forces resulting in an outer layer having elongated cells (which expressed collagen I resulting in enhanced tensile strength) and the inner silk-CS layers (due to the CS-conjugation to silk fibrous matrix) containing rounded chondrocytes (with expression of collagen II and GAG, leading to enhanced compressive strength).

expression of collagen II and GAG, leading to enhanced compressive strength (Figure 9). Further testing of these silk based constructs under controlled dynamic loading conditions would allow a more direct comparison of the tissue engineered constructs with the native disc tissue.

4. CONCLUSIONS

Our results showed that using a concentric lamellar architecture of silk fibrous scaffolds a cartilaginous gradient can be formed in the same construct, as a consequence of strategic decoration of silk fibroin fibers by chondroitin sulfate and hydrodynamic shear stress environment, to simulate anatomical features of outer and inner AF layers. The dynamic culture conditions enhanced the cellular metabolic activity and ECM deposition because of the flow-induced shear force, compared to the static culture. Inner regions enriched in GAG and collagen II were stiffer in compression, whereas the peripheral region was rich in collagen I and stiffer in tension. Therefore, the unique combination of chemical and physical parameters of engineered constructs and dynamic culture conditions could offer interesting possibilities to replicate the anatomical structure and composition gradient and function of intervertebral disc tissue.

AUTHOR INFORMATION

Corresponding Author

*E-mail: sghosh08@textile.iitd.ac.in.

Notes

The authors declare no competing financial interest.

ACKNOWLEDGMENTS

The authors would like to acknowledge the financial support from Indian Council of Medical Research project (09/NCD-1).

REFERENCES

(1) Roughley, P. J. *Spine (Phila Pa 1976)* **2004**, *29*, 2691−2699.
(2) Chou, A. I.; Bansal, A.; Miller, G. J.; Nicoll, S. B. *Spine (Phila Pa 1976)* **2006**, *3*, 1875−1881.
(3) Horner, H. A.; Roberts, S.; Bielby, R. C.; Menage, J.; Evans, H.; Urban, J. P. *Spine (Phila Pa 1976)* **2002**, *27*, 1018−1028.
(4) Bruehlmann, S. B.; Rattner, J. B.; Matyas, J. R.; Duncan, N. A. *J. Anat.* **2002**, *201*, 159−71.
(5) McNally, D. S.; Adams, M. A. *Spine (Phila Pa 1976)* **1992**, *17*, 66−73.
(6) Setton, L. A.; Chen, J. *J. Bone Jt. Surg. Am.* **2006**, *88*, 52−57.
(7) Baer, A. E.; Laursen, T. A.; Guilak, F.; Setton, L. A. *J. Biomech. Eng.* **2003**, *125*, 1−11.
(8) Shao, X.; Hunter, C. J. *J. Biomed. Mater. Res. A* **2007**, *82*, 701−710.
(9) Yang, L.; Kandel, R. A.; Chang, G.; Santerre, J. P. *J. Biomed. Mater. Res. A* **2008**, *91*, 1089−1099.
(10) Gruber, H. E.; Hoelscher, G.; Ingram, J. A.; Hanley, E. N. *Spine (Phila Pa 1976)* **2009**, *34*, 4−9.
(11) Reza, A. T.; Nicoll, S. B. *Ann. Biomed. Eng.* **2008**, *36*, 204−213.
(12) Wan, Y.; Feng, G.; Shen, F. H.; Laurencin, C. T.; Li, X. *Biomaterials* **2008**, *29*, 643−652.
(13) Bhattacharjee, M.; Miot, S.; Spagnoli, G.; Martin, I.; Ghosh, S.; Ray, A. R. *Proc. Indian Natl. Sci. Acad.* **2011**, *77*, 125−131.
(14) Bhattacharjee, M.; Miot, S.; Gorecka, A.; Singha, K.; Loparic, M.; Dickinson, S.; Das, A.; Bhavesh, N. S.; Ray, A. R.; Martin, I.; Ghosh, S. *Acta Biomater.* **2012**, *8*, 3313−3325.

(15) Das, S.; Pati, F.; Chameettachal, S.; Pahwa, S.; Ray, A. R.; Dhara, S.; Ghosh, S. *Biomacromolecules* **2013**, *14*, 311−321.
(16) Ignat'eva, N. Y.; Danilov, N. A.; Averkiev, S. V.; Obrezkova, M. V.; Lunin, V. V.; Sobol', E. N. *J. Anal. Chem.* **2007**, *62*, 51−57.
(17) Fonck, E.; Feigl, G. G.; Fasel, J.; Sage, D.; Unser, M.; Rüfenacht, D. A.; Stergiopulos, N. *Stroke* **2009**, *40*, 2552−2556.
(18) Pearce, R. H.; Grimmer, B. J. *Biochem. J.* **1976**, *157*, 753−763.
(19) Kääpä, E.; Holm, S.; Inkinen, R.; Lammi, M. J.; Tammi, M.; Vanharanta, H. *J. Spinal Disord.* **1994**, *7*, 296−306.
(20) Maeda, S.; Miyabayashi, T.; Yamamoto, J. K.; Roberts, G. D.; Lepine, A. J.; Clemmons, R. *M. J. Vet. Med. Sci.* **2001**, *63*, 1039−1043.
(21) Chang, G.; Kim, H. J.; Vunjak-Novakovic, G.; Kaplan, D. L.; Kandel, R. *J. Biomed. Mater. Res. A* **2010**, *92*, 43−51.
(22) Vunjak-Novakovic, G.; Martin, I.; Obradovic, B.; Treppo, S.; Grodzinsky, A.J.; Langer, R.; Freed, L.E. *J. Orthop. Res.* **1999**, *17*, 130−138.
(23) Smith, L. J.; Fazzalari, N. L. *J. Anat.* **2006**, *209*, 359−367.
(24) Yu, J.; Tirlapur, U.; Fairbank, J.; Handford, P.; Roberts, S.; Winlove, C. P.; Cui, Z.; Urban, J. *J. Anat.* **2007**, *210*, 460−475.
(25) Yu, J.; Winlove, P. C.; Roberts, S.; Urban, J. P. *J. Anat.* **2002**, *201*, 465−475.
(26) Hayes, A. J.; Smith, S. M.; Gibson, M. A.; Melrose, J. *Spine (Phila Pa 1976)* **2011**, *36*, 1365−1372.
(27) Tu, Y.; Weiss, A. S. *Biomacromolecules* **2008**, *9*, 1739−1744.
(28) Hayes, A. J.; Lord, M. S.; Smit, S. M.; Smith, M. M.; Whitelock, J. M.; Weiss, A. S.; Melrose, J. *Histochem. Cell Biol.* **2011**, *136*, 437−454.
(29) Marsano, A.; Millward-Sadler, S. J.; Salter, D. M.; Adesida, A.; Hardingham, T.; Tognana, E.; Kon, E.; Chiari-Grisar, C.; Nehrer, S.; Jakob, M.; Martin, I. *Osteoarthritis Cartilage* **2006**, *15*, 48−58.
(30) Marsano, A.; Wendt, D.; Quinn, T. M.; Sims, T. J.; Farhadi, J.; Jakob, M.; Heberer, M.; Martin, I. *Biorheology* **2006**, *43*, 553−560.
(31) Bueno, E. M.; Bilgen, B.; Barabino, G. A. *Tissue Eng., Part A* **2009**, *15*, 773−785.
(32) Marsano, A.; Wendt, D.; Raiteri, R.; Gottardi, R.; Stolz, M.; Wirz, D.; Daniels, A. U.; Salter, D.; Jakob, M.; Quinn, T. M.; Martin, I. *Biomaterials* **2006**, *27*, 5927−5934.
(33) Varghese, S.; Hwang, N. S.; Canver, A. C.; Theprungsirikul, P.; Lin, D W.; Elisseeff, J. *Matrix Biol.* **2008**, *27*, 12−21.
(34) Cowan, D. B.; Langille, B. L. *Curr. Opin. Lipidol.* **1996**, *7*, 94−100.
(35) Waldman, S. D.; Spiteri, C. G.; Grynpas, M. D.; Pilliar, R. M.; Kandel, R. A. *J. Orthop. Res.* **2003**, *21*, 590−596.
(36) Rannou, F.; Richette, P.; Benallaoua, M.; Francois, M.; Genries, V.; Korwin-Zmijowska, C.; Revel, M.; Corvol, M.; Poiraudeau, S. *J. Cell. Biochem.* **2003**, *90*, 148−157.
(37) Malaviya, P.; Nerem, R. M. *Tissue Eng.* **2002**, *8*, 581−590.
(38) Gooch, K. J.; Kwon, J. H.; Blunk, T.; Langer, R.; Freed, L. E.; Vunjak- Novakovic, G. *Biotechnol. Bioeng.* **2001**, *72*, 402−407.
(39) Bilgen, B.; Barabino, G. A. *Biotechnol. Bioeng.* **2007**, *98*, 282−294.
(40) Lindahl, G. E.; Chambers, R. C.; Papakrivopoulou, J.; Dawson, S. J.; Jacobsen, M. C.; Bishop, J. E.; Laurent, G. J. *J. Biol. Chem.* **2002**, *277*, 6153−6161.
(41) Bishop, J. E.; Lindahl, G. *Cardiovasc. Res.* **1999**, *42*, 27−44.
(42) Chen, S. J.; Yuan, W.; Mori, Y.; Levenson, A.; Trojanowska, M.; Varga, J. *J. Invest. Dermatol.* **1999**, *112*, 49−57.
(43) Xiea, J.; Hanb, Z. Y.; Matsuda, T. *Biochem. Biophys. Res. Commun.* **2006**, *344*, 1192−1199.
(44) Furukawa, T.; Ito, K.; Nuka, S.; Hashimoto, J.; Takei, H.; Takahara, M.; Ogino, T.; Young, M. F.; Shinomura, T. *Spine (Phila Pa 1976)* **2009**, *34*, 911−917.
(45) Melrose, J.; Ghosh, P.; Taylor, T. K. *J. Anat.* **2001**, *198*, 3−15.
(46) Martin, S. S.; Zorn, T. M. *Cell Mol. Biol.* **2003**, *49*, 673−678.
(47) Cs-Szabo, G.; Ragasa-San, J. D.; Turumella, V.; Masuda, K.; Thonar, E. J.; An, H. S. *Spine (Phila Pa 1976)* **2002**, *27*, 2212−2219.
(48) Ebara, S.; Iatridis, J. C.; Setton, L. A.; Foster, R. J.; Mow, V. C.; Weidenbaum, M. *Spine (Phila Pa 1976)* **1996**, *15*, 452−461.
(49) Urban, J. P. G.; Maroudas, A. *Connect Tissue Res.* **1981**, *9*, 1−10.
(50) Skaggs, D. L.; Weidenbau, M.; Iatridis, J. C.; Ratcliffe, A.; Mow, V. C. *Spine (Phila Pa 1976)* **1994**, *15*, 1310−1319.
(51) Chen, T.; Hilton, M. J.; Brown, E. B.; Zuscik, M. J.; Awad, H. A. *Biotechnol. Bioeng.* **2013**, *110*, 1476−1486.
(52) Chen, T.; Buckley, M.; Cohen, I.; Bonassar, L.; Awad, H. A. *Biomech. Model Mechanobiol.* **2012**, *11*, 689−702.